Probing Ground-State Phase Transitions through Quench Dynamics

Paraj Titum, Joseph T. Iosue, James R. Garrison, Alexey V. Gorshkov, and Zhe-Xuan Gong

Phys. Rev. Lett. **123**, 115701 — Published 11 September 2019

DOI: 10.1103/PhysRevLett.123.115701

Probing ground-state phase transitions through quench dynamics

Paraj Titum,[1,2] Joseph T. Iosue,[1,3] James R. Garrison,[1,2] Alexey V. Gorshkov,[1,2] and Zhe-Xuan Gong[4,1,2]

[1]*Joint Quantum Institute, NIST/University of Maryland, College Park, Maryland 20742, USA*
[2]*Joint Center for Quantum Information and Computer Science, NIST/University of Maryland, College Park, Maryland 20742, USA*
[3]*Massachusetts Institute of Technology, Cambridge, Massachusetts 02139, USA*
[4]*Department of Physics, Colorado School of Mines, Golden, Colorado 80401, USA*

(Dated: July 19, 2019)

The study of quantum phase transitions requires the preparation of a many-body system near its ground state, a challenging task for many experimental systems. The measurement of quench dynamics, on the other hand, is now a routine practice in most cold atom platforms. Here we show that quintessential ingredients of quantum phase transitions can be probed directly with quench dynamics in integrable and nearly integrable systems. As a paradigmatic example, we study global quench dynamics in a transverse-field Ising model with either short-range or long-range interactions. When the model is integrable, we discover a new dynamical critical point (DCP) with a nonanalytic signature in the *short-range correlators*. The location of the dynamical critical point matches that of the quantum critical point and can be identified using a finite-time scaling method. We extend this scaling picture to systems near integrability and demonstrate the continued existence of a dynamical critical point detectable at prethermal time scales. We quantify the difference in the locations of the dynamical and quantum critical points away from (but near) integrability. Thus, we demonstrate that this method can be used to approximately locate the quantum critical point near integrability. The scaling method is also relevant to experiments with finite time and system size, and our predictions are testable in near-term experiments with trapped ions and Rydberg atoms.

Introduction.—Experimental advances in isolating and controlling nonequilibrium quantum systems have brought within reach answers to many fundamental questions, including those related to thermalization, prethermalization, and many-body localization [1–6]. The exquisite control of complex quantum systems has become commonplace as a result of progress in various platforms, such as trapped ions [7, 8], ultracold atoms [9, 10], nitrogen-vacancy centers [11], Rydberg atoms [12], and others.

Among other interesting topics in nonequilibrium quantum many-body physics, phase transitions that emerge in the dynamics of isolated quantum systems have attracted significant theoretical and experimental interest [13–20]. There are two known types of dynamical phase transitions: (i) when a global order parameter (such as the Loschmidt echo) shows an abrupt change as a function of evolution time, or (ii) when a local order parameter measured after a sufficiently long time becomes nonanalytic as a function of some Hamiltonian parameter [14]. This latter type of dynamical phase transition is closely related to quantum phase transitions; the only difference is that the order parameter is measured in the quenched state instead of the ground state. It is thus natural to ask how this dynamical phase transition is related to a quantum phase transition. While difficult to answer, this question is not only of fundamental importance, but also motivates the idea of using dynamics to study quantum phase transitions. In fact, in many of the above-mentioned experimental platforms, cooling a system to its ground state can be a formidable task while performing a quench experiment is now a routine practice.

In this Letter, we first establish a strong connection between the quantum critical point and a new dynamical critical point (DCP) in a general class of integrable models, using the transverse-field Ising model (TFIM) as a paradigm. We show analytically that these critical points are identical and expect such behavior to generalize to other systems consisting of noninteracting particles [21]. This DCP has a nonanalytic signature in the long-time values of short-range, two-point correlation functions. Much of the previous work on the quench dynamics of the TFIM has focused on the behavior of long-range correlations [14, 18, 22–25], a common practice in studying equilibrium phase transitions. However, these correlations vanish in the thermodynamic limit for all nonzero field values due to the absence of long-range order at long time. Thus short-range correlations, often ignored due to the dominance of long-wavelength physics at low temperature, are important in identifying dynamical criticality and revealing its connections to quantum phase transitions.

Second, we show that analogous to the finite-size scaling analysis for identifying quantum critical points, one can perform a finite-time scaling analysis for obtaining the DCP. Intuitively, this can be understood because the evolution time controls the effective system size seen by short-range correlations as a result of emergent light cones. This finite-time scaling analysis is particularly favorable for quantum simulation experiments, as one does not need to create systems of different sizes or wait for a time much longer than the coherence time, and thus, allows for near-term experimental demonstration [12, 17].

Finally, we generalize our findings to systems that are nonintegrable by adding weak interactions. We show that the finite-time scaling predicts a DCP in the prethermal time scale. In general, the dynamical critical point will no longer coincide with the quantum critical point away from integrability. But, as shown by our analysis of the TFIM with next-nearest-neighbor and power-law decaying interactions, we expect the two transition points to be close to each other when in-

teractions are weak. As perturbation theory may not work for finding quantum critical points of weakly interacting systems, our findings provide an alternative and experimental way of locating such critical points.

We point out that some earlier works have considered similar ideas of studying quantum criticality via quench dynamics. For example, Ref. [26] studies the appearance of nonanalytic signatures in the periodically kicked Ising model, Refs. [21], and [27] discuss signatures in the quench dynamics for noninteracting topological phase transitions, Ref. [28] studies nonanalytic behavior in longitudinal magnetization, Ref. [29] studies energy absorption and Ref. [30] uses out-of-time-order correlators (OTOCs) to identify quantum phase transitions. However, our approach offers three unique advantages: (i) The short-range correlations are easy to measure experimentally, especially compared to the OTOC. (ii) Our approach is not restricted to exactly integrable systems. (iii) The finite-time scaling analysis we introduce provides a practical method to locate the dynamical critical point.

Model.—We consider two models for the quench Hamiltonian of L spins in one dimension: a transverse-field Ising model with next-nearest-neighbor or long-range interactions,

$$H_{\rm NNN} = -J\sum_{\langle i,j\rangle}\sigma_i^x\sigma_j^x - J\Delta\sum_{\langle\langle i,j\rangle\rangle}\sigma_i^x\sigma_j^x + B\sum_i\sigma_i^z, \quad (1)$$

$$H_{\rm LR} = -\sum_{i<j}J_{ij}^{(\alpha)}\sigma_i^x\sigma_j^x + B\sum_i\sigma_i^z, \quad (2)$$

where $\{\sigma_i^{x,y,z}\}$ denote the Pauli matrices and $\langle\cdots\rangle$ and $\langle\langle\cdots\rangle\rangle$ denote nearest and next-nearest neighbors, respectively. We will use periodic boundary conditions to ensure translation invariance unless otherwise noted. In the long-range Hamiltonian, the Ising coupling is defined as $J_{ij}^{(\alpha)} = J\left[\frac{1}{|i-j|^\alpha}+\frac{1}{|L-(i-j)|^\alpha}\right]$, which accounts for periodic boundary conditions [31]. We restrict to case of ferromagnetic interactions with J and $\Delta > 0$.

The quench and measurement protocol is shown schematically in Fig. 1(a). We initialize the system in a product state with all spins polarized in the Ising direction, $|\psi_{\rm in}\rangle = |\rightarrow\cdots\rightarrow\rangle$. This state is one of two degenerate ground states when $B = 0$. We focus on the dynamics under the quench Hamiltonian [see Eqs. (1) and (2)] of the nearest-neighbor, equal-time correlation function defined as

$$G(t) = \frac{1}{L}\sum_{\langle i,j\rangle}\langle\sigma_i^x(t)\sigma_j^x(t)\rangle_{\rm in}, \quad (3)$$

where $\langle\cdots\rangle_{\rm in}$ indicates the expectation value with respect to the initial state $|\psi_{\rm in}\rangle$ defined above, and the operators are written in the Heisenberg picture, $\sigma_i^x(t) = e^{iHt}\sigma_i^x e^{-iHt}$. We note that the dynamics of two-point correlators at longer distances independent of the system size (e.g. $\langle\sigma_i^x\sigma_{i+2}^x\rangle$) will be similar to $G(t)$. However, calculating such longer range correlations would require a more complicated analytical treatment.

Results at the integrable point.—Consider first the nearest-neighbor TFIM [$\Delta = 0$ in Eq. (1) or $\alpha = \infty$ in Eq. (2)]. In this case, the Hamiltonian is integrable and can be mapped to free fermions via a Jordan-Wigner transformation with the boundary condition determined by the particle number parity [32]. The quasiparticle dispersion is given by $\omega_q = 2\sqrt{B^2 - 2BJ\cos q + J^2}$, where q denotes momentum, and the Hamiltonian becomes $H = \sum_q \omega_q\gamma_q^\dagger\gamma_q$, where γ_q are the annihilation operators for the Bogoliubov quasiparticles. The time evolution is governed by a set of conserved densities of these quasiparticles, $I_q = \gamma_q^\dagger\gamma_q$. The ground state of this model exhibits a second-order phase transition with the critical point at $B = B_c^{\rm gs} \equiv J$.

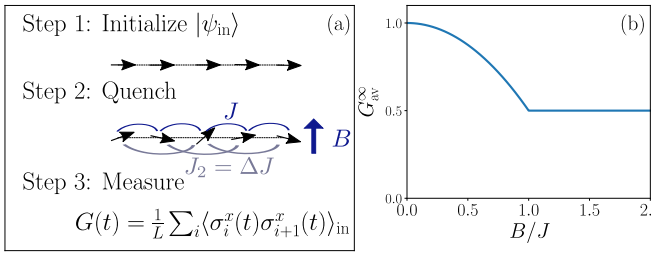

FIG. 1. (a) Schematic picture of the quench. We evolve the initial state $|\psi_{\rm in}\rangle$, which consists of all spins polarized in the Ising direction, for a time t under the Hamiltonian defined in Eq. (1) (shown) or Eq. (2). Then we measure the nearest-neighbor correlator $G(t)$ defined in Eq. (3). (b) The dependence of $G_{\rm av}^\infty$ on B as given by Eq. (5).

We calculate the time-averaged correlator $G_{\rm av}(t) \equiv \frac{1}{t}\int_0^t d\tilde{t}\, G(\tilde{t})$ to be [22, 32]

$$G_{\rm av}(t) = \frac{1}{L}\sum_q\frac{8B^2}{\omega_q^2}\left[\left(\frac{J}{B}-\cos q\right)^2 + j_0\left(2\omega_q t\right)\sin^2 q\right], \quad (4)$$

where $j_0(z) = \sin(z)/z$ is a spherical Bessel function of the first kind. The second term in Eq. (4) decays at long times: $j_0\left(2\omega_q t\right) \to 0$ as $t \to \infty$ (except when $\omega_q = 0$, in which case it is constant $\propto 1/L$). This means that the first term in Eq. (4) is the long-time stationary value. Taking the thermodynamic limit, we obtain an analytic expression for $G_{\rm av}(t)$,

$$G_{\rm av}^\infty \equiv \lim_{\substack{L\to\infty\\ t\to\infty}}\frac{1}{t}\int_0^t d\tilde{t}\, G(\tilde{t}) = \begin{cases} 1-\frac{B^2}{2J^2} & \text{if } B \le J \\ \frac{1}{2} & \text{if } B \ge J, \end{cases} \quad (5)$$

which has a nonanalyticity at $B = B_c^{\rm dy} \equiv J$. We refer to this nonanalytic point as a dynamical critical point (DCP). Note that the dynamical and ground state critical points are identical, $B_c^{\rm dy} = B_c^{\rm gs}$. This is because the nonanalyticity can be traced to the appearance of $1/\omega_q^2$ in the expression for $G_{\rm av}(t)$ [see Eq. (4)], which has a pole at $B = B_c^{\rm gs}$. In Fig. 1(b), we plot the long-time value of the correlator $G_{\rm av}^\infty$ [Eq. (5)], which exhibits a kink at $B = B_c^{\rm dy}$. Note that the expression for $G_{\rm av}^\infty$ is identical to that obtained from the Generalized Gibbs Ensemble (GGE) [33] for the TFIM.

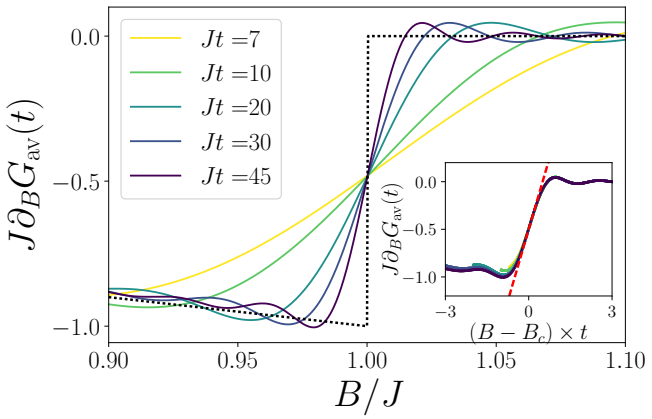

FIG. 2. Finite-time scaling for the integrable case. The first derivative of the correlator, $\frac{\partial}{\partial B}G_{\rm av}(t)$, exhibits a sharper jump across the transition ($B = B_c^{\rm dy} = J$) at later times. The curves are obtained by differentiating Eq. (4) with a system size $L = 100$ [32]. The curves at different times cross at the same point, thus revealing a DCP. The dotted line in black indicates the expected discontinuity in the derivative in the thermodynamic limit ($L \to \infty$) and at long times ($Jt \to \infty$). (Inset) We extract the time dependence by performing a scaling collapse after rescaling the magnetic field B by t. The scaling function near the critical point is linear, and is shown as a dashed red line.

The kink at the DCP is obtained after taking two limits in either order: (i) the infinite-time limit and (ii) the thermodynamic limit. In any realistic experiment, one can only measure $G_{\rm av}(t)$ at a finite time and a finite system size. In this case, $G_{\rm av}(t)$ is a smooth function of B, but we can nevertheless locate the DCP in the following way: We obtain the time-dependent derivative of $G_{\rm av}(t)$ with respect to B, i.e. $\partial_B G_{\rm av}(t)$ (see [32] for the explicit expression), and plot it in Fig. 2. We find the curves at different times cross at the same point up to a small correction $\propto \frac{1}{L}$, thus revealing a DCP. In fact, all the curves can be made to collapse into a single curve (shown in the inset) by rescaling the field B by Jt. The expression for $\partial_B G_{\rm av}(t)$ near the DCP takes the form of a universal scaling function, $\partial_B G_{\rm av}(t) = \frac{1}{J} f((B - B_c^{\rm dy})t)$. To lowest order in the distance from the critical point (given by $\epsilon = B - B_c^{\rm dy}$), the scaling function is $f(\epsilon t) = -\frac{1}{2} + \epsilon t$ [32]. Note that this finite-time scaling function is very similar to the finite-size scaling function of the long-time correlator near the critical point, with t playing the role of $L/(3J)$ [32]. The finite-time scaling analysis thus allows us to locate the position of the DCP, and in this (integrable) case, also the quantum critical point.

Let us discuss the generality of this result for different initial states. For an arbitrary initial state, $G_{\rm av}^{\infty}$ is given by

$$G^{\infty}_{\rm av,arbitrary} = \frac{1}{L}\sum_q \frac{2(J - B\cos q)}{\omega_q}\left[1 - 2\langle I_q\rangle_{\rm in}\right], \quad (6)$$

where $\langle I_q\rangle_{\rm in}$ is the expectation value of the conserved quasiparticle densities in the initial state. It is clear from this expression that the nonanalyticity which results from a gapless ω_q will survive for arbitrary initial states unless the form of $\left[1 - 2\langle I_q\rangle_{\rm in}\right]$ cancels off the $1/\omega_q$ singularity at $q = 0$. A generic pure initial state is thus expected to lead to the same dynamical critical behavior. In the Supplemental Material, we show explicitly the robustness of the dynamical criticality to perturbations of the initial state, particularly under realistic experimental conditions [32]. Interestingly, a thermal initial state given by the density matrix $\rho_{\rm th} = e^{-\beta H}/\operatorname{tr}\left[e^{-\beta H}\right]$ is an exception. This is because in this case, $\langle I_q\rangle_{\rm in} = \operatorname{tr}(\rho_{\rm th} I_q) = \frac{1}{2}\left[1 - \tanh\left(\frac{\beta\omega_q}{2}\right)\right] \approx \frac{1}{2}\left(1 - \frac{\beta}{2}\omega_q\right)$ when $\omega_q \to 0$ and thus $G_{\rm av}^{\infty}$ becomes an analytic function of B. This is consistent with the well-known fact that the 1D nearest-neighbor TFIM does not have a thermal phase transition. We note that this dynamical criticality is present in other noninteracting Hamiltonians which have single-particle dispersion $\sim \omega_q$ and exhibit phase transitions.

Results away from integrability.—Now, let us consider the TFIM with either an additional next-nearest-neighbor interaction [$\Delta \neq 0$ in Eq. (1)] or long-range interactions [any finite α in Eq. (2)]. Assuming the Eigenstate Thermalization Hypothesis (ETH) [3] holds, we expect local observables, including $G(t)$, to thermalize at sufficiently long times. For any finite value of Δ or $\alpha > 2$, it has been established that the TFIM does not exhibit a thermal phase transition [34, 35]. Thus, once the system fully thermalizes, any measured observable has to be analytic and thus, it should no longer have a DCP. (The situation with $\alpha < 2$ is beyond the scope of this Letter due to the strong effects of long-range interactions that could break ETH [14].)

However, as recently shown by Refs. [18, 19], it is possible to still observe a dynamical phase transition when local observables have not yet thermalized but instead have reached prethermal values. This is the case here when Δ is small or α is large, so that the Hamiltonian is nearly integrable and prethermalization is expected to occur [36, 37]. The DCP in the prethermal regime is also relevant for experiments in the near future, as the thermalization timescale is likely to be far beyond the experimental coherence time [8, 9, 38].

We now show that our finite-time scaling method can also reveal DCPs in the prethermal regime of nearly integrable systems. We calculate dynamics of Eq. (1) with $\Delta \neq 0$ and Eq. (2) with finite α numerically due to the lack of analytic solutions. Using a split-operator decomposition (using fourth-order Suzuki-Trotter expansion) coupled with a Walsh-Hadamard transform, we calculate dynamics for up to $L = 25$ spins (see [32] for technical details). In Figs. 3(a) and (b) we plot the time dependence of the derivative of $G_{\rm av}(t)$ for $\Delta = 0.1$ and $\alpha = 6$ respectively. Remarkably, the curves at different times still cross at one point, which we identify as the DCP $B_c^{\rm dy}$. We note that this DCP survives at intermediate time scales as a consequence of prethermalization. These curves will also collapse almost perfectly on top of each other using a scaling function $\partial_B G_{\rm av}(t) = \frac{1}{J}\tilde{f}\left((B - B_c^{\rm dy})t\right)$ [32]. While the scaling function depends on the model, we expect the variables of the scaling function are universal and inde-

pendent of microscopic details.

In the integrable TFIM, we showed that the DCP $B_c^{\rm dy}$ coincides with the ground-state critical point $B_c^{\rm gs}$. It is natural to ask whether this is still the case for the above-calculated models near integrability. To locate the quantum critical point, we compute the Binder cumulant [39], $\mathcal{U}_4^{\rm gs} = 1 - \frac{\langle M^4\rangle_{\rm gs}}{3\langle M^2\rangle_{\rm gs}^2}$ (where $M = \frac{1}{L}\sum_i \sigma_i^x$ and $\langle\cdots\rangle_{\rm gs}$ denotes the ground-state expectation value) using a DMRG algorithm for a system with open boundary conditions and sizes ranging from $L = 30$ to $L = 140$. We identify the quantum critical point using a finite-size scaling method as shown in Figs. 3(c) and (d). It is found that $B_c^{\rm dy}$ is close, but not identical, to $B_c^{\rm gs}$ at both $\Delta = 0.1$ and $\alpha = 6$.

While we cannot make a conclusive statement about whether $B_c^{\rm dy}$ agrees with $B_c^{\rm gs}$ in the thermodynamic limit based on finite-size numerical calculations, we argue that $B_c^{\rm dy}$ and $B_c^{\rm gs}$ should in general be different but close to each other when near integrability. To support this argument, we perform a self-consistent mean-field calculation [40] for Eq. (1) with $\Delta = 0.1$ to identify both $B_c^{\rm dy}$ and $B_c^{\rm gs}$ in the thermodynamic limit [32]. The next-nearest-neighbor spin interaction translates to a perturbative two-particle interaction of the Jordan-Wigner fermions. The essence of the self-consistent calculation is to approximate this interaction by effective single-particle hoppings and on-site energies. This makes the Hamiltonian noninteracting, with the quench dynamics given by an effective GGE. The parameters of this effective Hamiltonian must be determined self-consistently from the expectation values of different correlation functions. These expectation values may be considered either in the ground state or the effective GGE corresponding to the quench from some initial state. While the former determines the quantum critical point $B_c^{\rm gs}$ [40], we claim that the latter captures the DCP $B_c^{\rm dy}$. Therefore, it is natural to expect a difference in the locations of the dynamical and quantum critical points.

The self-consistent mean-field calculation should be asymptotically exact as $\Delta \to 0$. We find that to first order in Δ, $B_c^{\rm dy} \approx J\left(1 + \frac{3}{2}\Delta\right)$ and $B_c^{\rm gs} \approx J\left(1 + \frac{16}{3\pi}\Delta\right)$ [32]. For $\Delta = 0.1$, these predict $B_c^{\rm dy} \approx 1.15$ and $B_c^{\rm gs} \approx 1.168$, agreeing very well with numerics in Figs. 3(a) and (c). We have further confirmed the accuracy of these predictions for Δ up to 0.3 [32]. For the larger values of Δ, it is clear that $B_c^{\rm dy} \neq B_c^{\rm gs}$, but they are close in magnitude when $\Delta \approx 0$. Thus, near integrability, the dynamical critical field can be used to approximately locate the quantum critical point.

Discussion.—Our results are relevant to experiments in trapped ions [17] and Rydberg atoms [12], where dynamics of the TFIM can be readily probed. As an example, we numerically obtain the dynamics for the $\alpha = 6$ TFIM, which models Rydberg atoms interacting via van der Waals type long-range interactions [41]. We find that the numerically obtained DCP $B_c^{\rm dy} \approx 1.028J$ shown in Fig. 3(b) is very close to the ground-state critical point $B_c^{\rm gs} \approx 1.03J$ obtained from finite-size scaling shown in Fig. 3(d). We emphasize that the DCP is identified by our finite-time scaling method for a system size

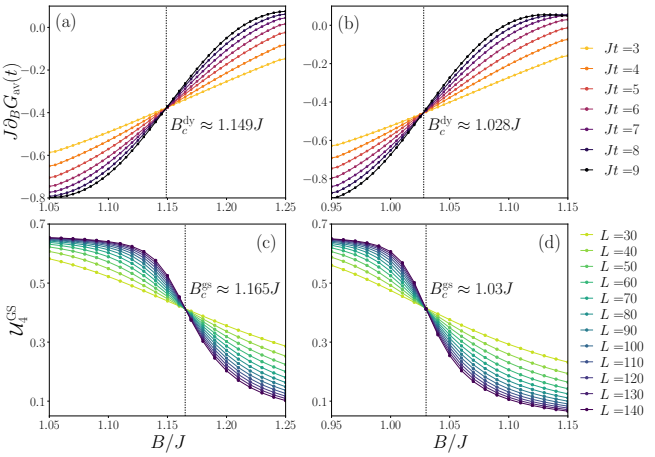

FIG. 3. Comparison between the finite-time scaling of the time-averaged nearest-neighbor correlator $G_{\rm av}(t)$ and the ground-state Binder cumulant $\mathcal{U}_4^{\rm gs}$. The first column [panels (a) and (c)] corresponds to the TFIM with next-nearest-neighbor interaction $\Delta = 0.1$ [Eq. (1)], while the second column [panels (b) and (d)] corresponds to the TFIM with long-range interaction $\alpha = 6$ [Eq. (2)]. The finite-time scaling of the quench dynamics is shown in the first row, and the finite-size scaling for the ground state is shown in the second row. The DCPs ($B_c^{\rm dy}$) identified in (a) and (b) using finite-time scaling are close but different from the locations of the quantum critical points ($B_c^{\rm gs}$) identified in (c) and (d). The ground-state simulations were done using a DMRG algorithm with bond dimension $\chi = 32$.

of only 25 spins and an evolution time of only $9/J$, which are well within the current experimental record for the system size and coherence time [12]. As a result, we believe our method is a paradigmatic example of what Near-term Intermediate Scale Quantum (NISQ) simulators can do: learn new physics that cannot be obtained by classical simulation, yet without the need for a very large number of qubits, very low error, and very long coherence times.

Our work opens up several interesting questions for future consideration: (i) How should one classify the observed DCP? We note that the DCP identified using $G(t)$ as an "order parameter" does not represent a conventional symmetry-breaking phase transition, because for both $B < B_c^{\rm dy}$ and $B > B_c^{\rm dy}$, the quenched state does not spontaneously break the Ising symmetry and become ferromagnetically ordered. (ii) Is finite-time scaling a general method for identifying DCPs? We believe that for generic, short-range interacting systems, finite-time scaling serves the purpose of finite-size scaling for finding the quantum critical point due to the emergence of linear light cones [42]. However, when interactions become long-range, the linear light cone may no longer exist [43, 44] and it remains unclear when the finite-time scaling method fails. (iii) Could the link between dynamical and quantum critical points established here be generalized to other integrable and nearly integrable systems, such as systems solvable by Bethe ansatz or many-body localized systems? Here the link is provided by the single-particle spectrum that governs both equilibrium and nonequilibrium

physics, but what happens when the single-particle spectrum is less relevant? Is there evidence of this dynamical criticality in nonintegrable models? (iv) Could there be similar links between dynamical phase transitions and phase transitions in excited eigenstates? This is particularly relevant in many-body localized systems [45]. (v) Can the prethermal DCP be predicted using other theoretical methods such as the kinetic equations using time-dependent GGEs [46, 47] or Keldysh field theory?

Acknowledgments.—We thank John Bollinger, Lincoln Carr, Fabian Essler, Mohammad Maghrebi, Tomaž Prosen, Marcos Rigol, Somendra M. Bhattacharjee, Sthitadhi Roy, and Soonwon Choi for useful discussions. The authors have been financially supported by the NSF Ideas Lab on Quantum Computing, ARO, AFOSR, NSF PFC at JQI, ARO MURI, ARL CDQI, the DOE ASCR Quantum Testbed Pathfinder program, and the DOE BES Materials and Chemical Sciences Research for Quantum Information Science program. P.T. and J.R.G. acknowledge support from the NIST NRC Research Postdoctoral Associateship Award. J.R.G. performed his work in part at the Aspen Center for Physics, which is supported by National Science Foundation grant PHY-1607611. Z.X.G. acknowledges the start-up fund support from Colorado School of Mines. This research was supported in part by the National Science Foundation under Grant No. NSF PHY-1748958. This work used the Extreme Science and Engineering Discovery Environment (XSEDE), which is supported by National Science Foundation grant number ACI-1548562. Specifically, it used the Bridges system, which is supported by NSF award number ACI-1445606, at the Pittsburgh Supercomputing Center (PSC) [48, 49]. The authors acknowledge the University of Maryland supercomputing resources (http://hpcc.umd.edu) made available for conducting the research reported in this Letter.

[1] J. M. Deutsch, Phys. Rev. A **43**, 2046 (1991).
[2] M. Srednicki, Phys. Rev. E **50**, 888 (1994).
[3] M. Srednicki, J. Phys. A **32**, 1163 (1999).
[4] M. Rigol, V. Dunjko, and M. Olshanii, Nature (London) **452**, 854 (2008).
[5] H. Kim, T. N. Ikeda, and D. A. Huse, Phys. Rev. E **90**, 052105 (2014).
[6] J. R. Garrison and T. Grover, Phys. Rev. X **8**, 021026 (2018).
[7] P. Richerme, Z.-X. Gong, A. Lee, C. Senko, J. Smith, M. Foss-Feig, Spyridon Michalakis, A. V. Gorshkov, and C. Monroe, Nature **511**, 198 (2014).
[8] B. Neyenhuis, J. Zhang, P. W. Hess, J. Smith, A. C. Lee, P. Richerme, Z.-X. Gong, A. V. Gorshkov, and C. Monroe, Sci. Adv. **3**, e1700672 (2017).
[9] T. Kinoshita, T. Wenger, and D. S. Weiss, Nature **440**, 900 (2006).
[10] M. Schreiber, S. S. Hodgman, P. Bordia, H. P. Luschen, M. H. Fischer, R. Vosk, E. Altman, U. Schneider, and I. Bloch, Science **349**, 842 (2015).
[11] S. Choi, J. Choi, R. Landig, G. Kucsko, H. Zhou, J. Isoya, F. Jelezko, S. Onoda, H. Sumiya, V. Khemani, C. von Keyserlingk, N. Y. Yao, E. Demler, and M. D. Lukin, Nature (London) **543**, 221 (2017).
[12] H. Bernien, S. Schwartz, A. Keesling, H. Levine, A. Omran, H. Pichler, S. Choi, A. S. Zibrov, M. Endres, M. Greiner, V. Vuletić, and M. D. Lukin, Nature (London) **551**, 579 (2017).
[13] M. Heyl, A. Polkovnikov, and S. Kehrein, Phys. Rev. Lett. **110**, 135704 (2013).
[14] B. Žunkovič, M. Heyl, M. Knap, and A. Silva, Phys. Rev. Lett. **120**, 130601 (2018).
[15] M. Heyl, Rep. Prog. Phys. **81**, 054001 (2018).
[16] P. Jurcevic, H. Shen, P. Hauke, C. Maier, T. Brydges, C. Hempel, B. P. Lanyon, M. Heyl, R. Blatt, and C. F. Roos, Phys. Rev. Lett. **119**, 080501 (2017).
[17] J. Zhang, G. Pagano, P. W. Hess, A. Kyprianidis, P. Becker, H. Kaplan, A. V. Gorshkov, Z.-X. Gong, and C. Monroe, Nature **551**, 601 EP (2017).
[18] J. C. Halimeh, V. Zauner-Stauber, I. P. McCulloch, I. de Vega, U. Schollwöck, and M. Kastner, Phys. Rev. B **95**, 024302 (2017).
[19] J. C. Halimeh and V. Zauner-Stauber, Phys. Rev. B **96** (2017).
[20] I. Homrighausen, N. O. Abeling, V. Zauner-Stauber, and J. C. Halimeh, Phys. Rev. B **96** (2017).
[21] S. Roy, R. Moessner, and A. Das, Phys. Rev. B **95**, 041105 (2017).
[22] P. Calabrese, F. H. L. Essler, and M. Fagotti, Phys. Rev. Lett. **106**, 227203 (2011).
[23] P. Calabrese, F. H. L. Essler, and M. Fagotti, J. Stat. Mech. Theory Exp. **2012**, P07016 (2012).
[24] P. Calabrese, F. H. L. Essler, and M. Fagotti, J. Stat. Mech. Theory Exp. **2012**, P07022 (2012).
[25] M. Karl, H. Cakir, J. C. Halimeh, M. K. Oberthaler, M. Kastner, and T. Gasenzer, Phys. Rev. E **96**, 022110 (2017).
[26] T. Prosen, Prog. Theor. Phys. Supplement **139**, 191 (2000).
[27] M. Tarnowski, F. Nur Ünal, N. Fläschner, B. S. Rem, A. Eckardt, K. Sengstock, and C. Weitenberg, arXiv:1709.01046.
[28] Y. Li, M. Huo, and Z. Song, Phys. Rev. B **80**, 054404 (2009).
[29] S. Bhattacharyya, S. Dasgupta, and A. Das, Scientific Reports **5**, 16490 (2015).
[30] M. Heyl, F. Pollmann, and B. Dóra, Phys. Rev. Lett. **121**, 016801 (2018).
[31] A. W. Sandvik, Phys. Rev. E **68**, 056701 (2003).
[32] See Supplemental Material, which includes Refs. [50–54], for additional details.
[33] L. Vidmar and M. Rigol, J. Stat. Mech. Theory Exp. **6**, 064007 (2016).
[34] S. Sachdev, *Quantum Phase Transitions*, 2nd ed. (Cambridge University Press, 2011).
[35] A. Dutta and J. K. Bhattacharjee, Phys. Rev. B **64**, 184106 (2001).
[36] T. Mori, T. N. Ikeda, E. Kaminishi, and M. Ueda, J. Phys. B **51**, 112001 (2018).
[37] T. Langen, T. Gasenzer, and J. Schmiedmayer, J. Stat. Mech. Theory Exp. **2016**, 064009 (2016).
[38] M. Gring, M. Kuhnert, T. Langen, T. Kitagawa, B. Rauer, M. Schreitl, I. Mazets, D. A. Smith, E. Demler, and J. Schmiedmayer, Science **337**, 1318 (2012).
[39] K. Binder, Z. Phys. B **43**, 119 (1981).
[40] P. Sen and B. K. Chakrabarti, Phys. Rev. B **43**, 13559 (1991).
[41] M. Saffman, T. G. Walker, and K. Mølmer, Rev. Mod. Phys. **82**, 2313 (2010).
[42] E. H. Lieb and D. W. Robinson, Comm. Math. Phys. **28**, 251 (1972).
[43] M. Foss-Feig, Z.-X. Gong, C. W. Clark, and A. V. Gorshkov,

Phys. Rev. Lett. **114**, 157201 (2015).
[44] Z. Eldredge, Z.-X. Gong, J. T. Young, A. H. Moosavian, M. Foss-Feig, and A. V. Gorshkov, Phys. Rev. Lett. **119**, 170503 (2017).
[45] D. A. Huse, R. Nandkishore, V. Oganesyan, A. Pal, and S. L. Sondhi, Phys. Rev. B **88**, 014206 (2013).
[46] L. D'Alessio, Y. Kafri, A. Polkovnikov, and M. Rigol, Adv. Phys. **65**, 239 (2016).
[47] B. Bertini, F. H. L. Essler, S. Groha, and N. J. Robinson, Phys. Rev. Lett. **115**, 180601 (2015).
[48] J. Towns, T. Cockerill, M. Dahan, I. Foster, K. Gaither, A. Grimshaw, V. Hazlewood, S. Lathrop, D. Lifka, G. D. Peterson, R. Roskies, J. R. Scott, and N. Wilkins-Diehr, Comput. Sci. Eng. **16**, 62 (2014).
[49] N. A. Nystrom, M. J. Levine, R. Z. Roskies, and J. R. Scott, in *Proceedings of the 2015 XSEDE Conference: Scientific Advancements Enabled by Enhanced Cyberinfrastructure*, XSEDE '15 (ACM, New York, NY, USA, 2015) pp. 30:1–30:8.
[50] A. Lakshminarayan and V. Subrahmanyam, Phys. Rev. A **71**, 062334 (2005).
[51] M. Frigo and S. G. Johnson, Proc. IEEE **93**, 216 (2005), special issue on "Program Generation, Optimization, and Platform Adaptation".
[52] M. Suzuki, Phys. Lett. A **146**, 319 (1990).
[53] D. W. Berry, G. Ahokas, R. Cleve, and B. C. Sanders, Commun. Math. Phys. **270**, 359 (2007).
[54] A. M. Childs, D. Maslov, Y. Nam, N. J. Ross, and Y. Su, arXiv:1711.10980.